J Mater Sci: Mater Electron (2011) 22:1313–1320
DOI 10.1007/s10854-011-0306-0

Barrier/bonding layers on bismuth telluride (Bi_2Te_3) for high temperature thermoelectric modules

Wen P. Lin · Daniel E. Wesolowski · Chin C. Lee

Received: 20 August 2010 / Accepted: 14 December 2010 / Published online: 26 January 2011

Abstract In this research, a fundamental study is conducted to identify the materials and develop the processes for producing barrier/bonding composite on Bi_2Te_3 for high temperature thermoelectric applications. The composite must meet four basic requirements: (a) prevent interdiffusion between the electrode material, for our design, silver(Ag) and Bi_2Te_3, (b) bond well to Bi_2Te_3, (c) bond well to Ag electrode, and (d) do not themselves diffuse into Bi_2Te_3. The composites investigated include palladium (Pd), nickel/gold (Ni/Au), Ag, and titanium/gold (Ti/Au). After annealing at 250 °C for 200 h, only the Ti/Au design meets all four requirements. The thickness of Ti and Au, respectively, is only 100 nm. Other than meeting these four requirements, the Ti/Au layers exhibit excellent step coverage on the rough Bi_2Te_3 surface even after the annealing process.

1 Introduction

Bismuth telluride (Bi_2Te_3) is a narrow band gap semiconductor with trigonal unit cell. It was first investigated as a thermoelectric (TE) material in 1950s [1–3]. The TE power generator uses Seebeck effect to convert temperature gradient ΔT into electrical power. The voltage produced is given by $V = \alpha\Delta T$, where α is Seebeck coefficient. Conversely, the TE cooler uses the Peltier effect to convert electrical power into temperature gradient by transporting heat from cold side to hot side. The heat transported is given by $Q_p = \pi I$, where I is the current and π is the Peltier coefficient. Bi_2Te_3 is so far the most popular TE material. Alloying with Sb_2Te_3 and Bi_2Se_3 can control carrier concentrations alongside a reduction in lattice thermal conductivity [4]. It can also improve the figure-of-merit, $Z = \alpha^2 (\sigma T/\lambda)$, where σ is the electrical conductivity and λ is its thermal conductivity. Bismuth-based alloys with antimony, tellurium, and selenium are referred to as low-temperature materials with Z around $2 \sim 4 \times 10^{-3}$ K^{-1} and can be used at temperature up to 450 K [5]. For temperature from 450 to 850 K, the most common thermoelectric material is lead telluride. At even higher temperature, silicon germanium alloys can operate up to 1,300 K [4, 5]. Z of lead telluride and silicon germanium alloy are below 2×10^{-3} K^{-1} [5]. Most TE devices on the market are made of Bi_2Te_3-based alloys.

A TE cooler or generator, portrayed in Fig. 1, is constructed of an array of p-type and n-type TE columns bonded between two ceramic plates [6]. These columns are connected electrically in series to form a chain of p-n junctions but thermally in parallel. Solder is employed to bond the TE columns to the ceramic plates. TE modules on the market have a maximum operating temperature of 80 °C on the hot side [7]. This constraint prohibits numerous applications and economic opportunities where higher operation temperature is required. An example is to cool the transistor in the front-end amplifier of an outdoor wireless communications base station to reduce its noise. Another example is to cool the front-end photodiode of a military laser range-finding receiver to increase its sensitivity. The 80 °C limit is imposed by severe diffusion of

W. P. Lin (✉) · C. C. Lee
Electrical Engineering and Computer Science,
Materials and Manufacturing Technology,
University of California, Irvine, CA 92697-2660, USA
e-mail: michellelin.tw@gmail.com

D. E. Wesolowski
Power Sources Technology Group, Sandia National Laboratories, Albuquerque, NM 87185, USA
e-mail: dewesol@sandia.gov

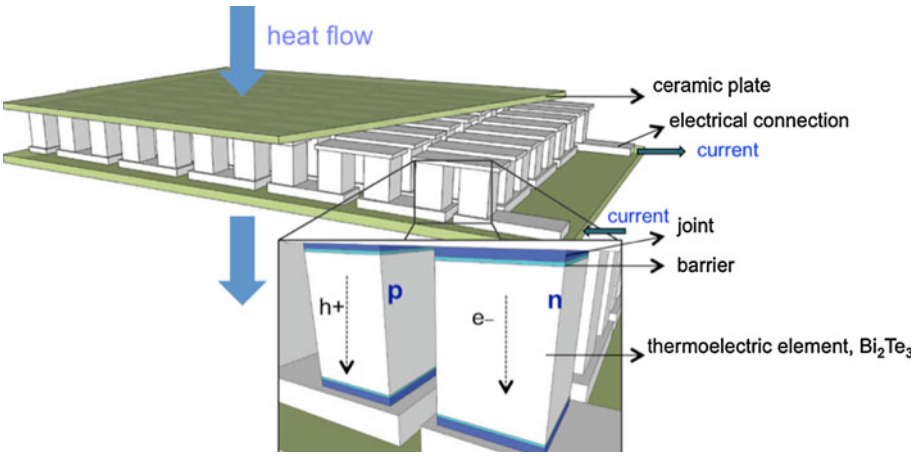

Fig. 1 The structure of a TE module

solder material into the TE materials rather than by TE materials themselves. The melting points of TE materials Bi_2Te_3, Sb_2Te_3, and Bi_2Se_3 are 585 °C [8], 618 °C [9], and 706 °C [10], respectively. Therefore, to extend the operating temperature to 150 °C, solder diffusion at high temperature must be stopped. Accordingly, high temperature bonding/barrier layers must be investigated and identified.

Several groups had studied diffusion barrier for Bi_2Te_3 and copper (Cu) interconnect. Few showed positive results. In one study, Ni was used as a diffusion-barrier for tin (Sn) in both $(Bi,Sb)_2Te_3$ and $Bi_2(Te,Se)_3$ [11]. Ni diffuses into $Bi_2(Te,Se)_3$ by several microns during the soldering process. Ni was also found to diffuse into $Bi_2(Te,Se)_3$ and form a nickel telluride interfacial region after heat treatment at 200 °C [12]. In another study, Ni-7% vanadium (V), Pd and platinum (Pt) films were used but failed to prevent inter-diffusion between Cu and Bi_2Te_3 after annealing at 200 °C for a few hours [13]. It is clear that several research groups had searched for diffusion barrier on Bi_2Te_3-based compounds. So far, the best barrier design can sustain 200 °C only for a few hours.

The objective of this research is to design and develop barrier/bonding composite that can sustain annealing at 250 °C for 200 h. The composite is fabricated between Bi_2Te_3-based compound and Ag electrode. One surface of the composite must bond to Bi_2Te_3-compound and the other surface must bond to Ag. Furthermore, it must prevent Ag atoms from diffusing into Bi_2Te_3 and prevent Bi_2Te_3 from diffusing into Ag electrode. Ag rather than Cu is chosen as the electrode material because it has the highest electrical conductivity and thermal conductivity among metals. To identify the right bonding/barrier materials and processes, we went through a systematic study, starting with Pd, followed by Ni/Au, Ag, and Ti/Au. Some preliminary results were presented in [14]. In this paper, we report more complete analyses and results. Additional information obtained includes: extensive 250 °C annealing data of Ti/Au barrier/bonding layer from 10 to 200 h, Ag surface morphology and adhesion on different barrier layers, SEM/EDX analyses on inter-diffused regions, and discussion on compound formation in inter-diffused regions.

In what follows, experimental design and procedure are presented. Experimental results are reported and discussed. A short summary is then given. For convenience, all chips made of Bi_2Te_3 and related alloys are referred to as Bi_2Te_3 chips.

2 Experimental design and procedure

Hot-pressed p- and n-type Bi_2Te_3 ingots were acquired from a commercial vendor. They are usually manufactured starting with bismuth antimony, selenium and tellurium shot of 99.999% purity. An alloying process converts the pure elements into compound of designed composition. Powdered alloys are extruded at a temperature between 400 and 500 °C [15]. They are then cut into 8mm × 8mm × 1 mm chips. The composition of n-type alloy is $(Bi_{0.95}Sb_{0.05})_2(Te_{0.95}Se_{0.05})_3$ and that of p-type alloy is $(Bi_{0.2}Sb_{0.8})_2Te_3$. The room temperature figures of merit are up to 3.3×10^{-3} K^{-1} for p-type alloys and 2.85×10^{-3} K^{-1} for n-type alloys [15]. The coefficient of thermal expansion (CTE) of Bi_2Te_3 is 16.4 ppm/ °C. The Bi_2Te_3 chips are thoroughly cleaned and baked at 120 °C for 30 min for dehydration.

Figure 2 portrays the structure of the barrier/bonding layers on Bi_2Te_3 chips with Ag as the electrode. The Ag electrode can be connected to the ceramic plate by soldering or other bonding means. The Ag layer is fabricated by an electroplating process. A thickness range of 10–20 μm is used. To search for bonding/barrier layers, we start with Pd because it has long been used in commercial TE cooling modules. Ni/Au, Ag, and Ti/Au are then studied. To produce a few microns of Pd, Ni/Au, and Ag layers, respectively, on Bi_2Te_3 chips, electroplating processes are employed. For depositing Ti films, we are not able to find a

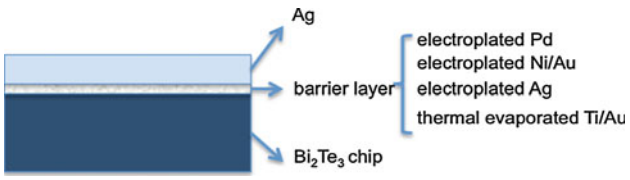

Fig. 2 Structure of barrier/bonding layers on a Bi_2Te_3 chip

plating solution. Thus, the Ti/Au layers are deposited by electron beam thermal evaporation in one vacuum cycle in 1×10^{-6} torr vacuum. The Ti layer is expected to bond to Bi_2Te_3 chips while the Au layer protects the Ti layer against oxidation.

The samples fabricated are cut in cross section and polished for examinations by optical microscope, scanning electron microscope (SEM) and EDX analysis. Some samples are annealed at 250 °C for 200 h prior to the cutting and polishing processes.

3 Experimental results and discussion

3.1 Pd barrier/bonding layer

The Bi_2Te_3 chips were coated with 1 μm Pd by electroplating process. Figure 3a and b show the SEM images of Pd surface on Bi_2Te_3 at low and high magnification, respectively. The surface of Pd is smooth and bonds well to Bi_2Te_3. The Pd grain size is less than 100 nm. The samples were then plated with 10 μm Ag and annealed at 250 °C for 10 h. After annealing, the Ag layer still adheres to the Pd layer which also bonds to the Bi_2Te_3 chip. To further study whether the Pd layer can sustain stresses induced by

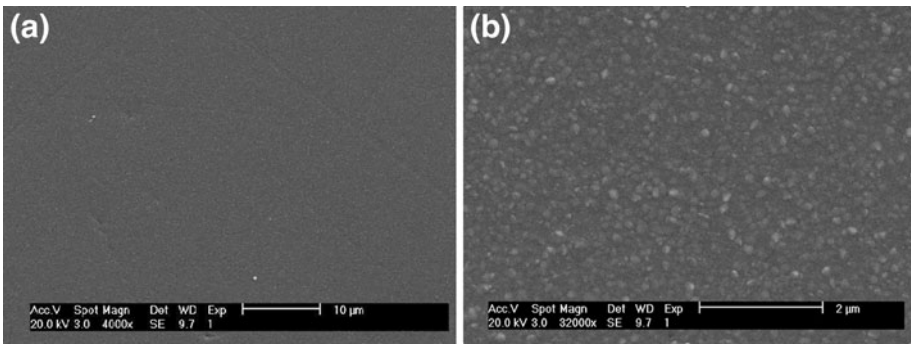

Fig. 3 SEM images of 1 μm Pd plated on Bi_2Te_3 at **a** low magnification and **b** high magnification

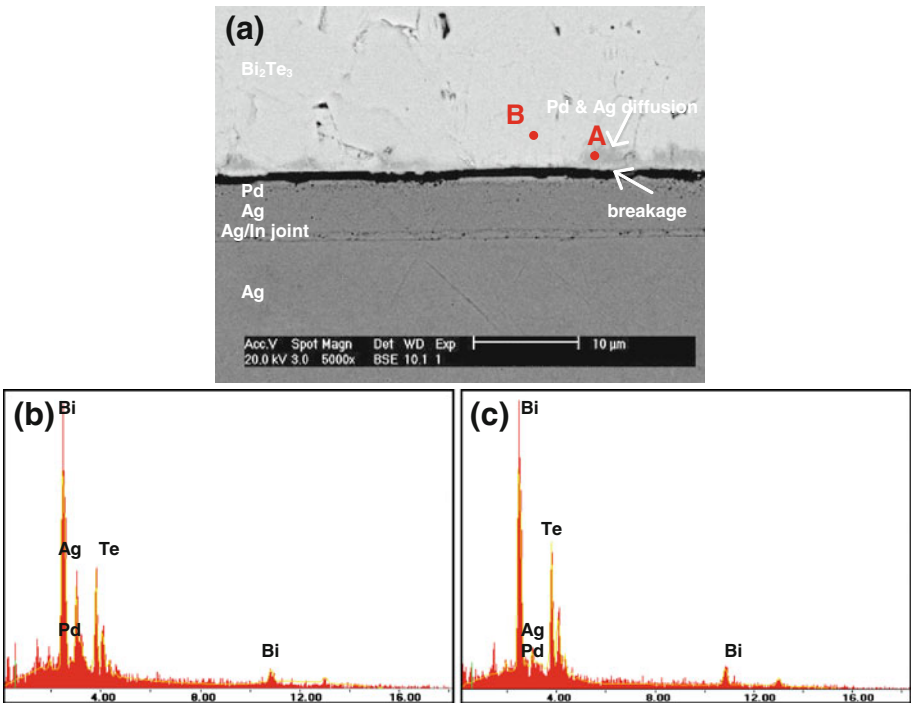

Fig. 4 SEM and EDX evaluations of Bi_2Te_3/Pd (1 μm)/Ag (10 μm) bonded to alumina/Ag (60 μm)/In (5 μm)/Ag (100 nm) structure to produce an Ag-In joint. **a** Cross section SEM image. The alumina substrate is not shown here. The Bi_2Te_3/Pd (1 μm)/Ag (10 μm) sample was annealed at 250 °C for 10 h. The Bi_2Te_3 chip broke off along the Bi_2Te_3-Pd interface after the bonding due to CTE mismatch with alumina substrate. Significant Pd and Ag have diffused into Bi_2Te_3 after the annealing and prior to bonding. **b** EDX spectra at location A, **c** EDX spectra at location B. EDX quantitative data are presented in Table 1

Table 1 EDX quantitative data at locations A and B marked in Fig. 4a

Location	At.%			
	Bi	Te	Pd	Ag
A	8	31	5	54
B	14	78	1	7

The accelerating voltage is 20 kV

CTE mismatch while bonding on alumina substrate, the Bi_2Te_3/Pd/Ag samples were plated with a layer of 5 μm In and a thin Ag cap layer. The Bi_2Te_3 chips were bonded to alumina substrates. The bonded structure was cut in cross section and polished for evaluations. Figure 4a exhibits a cross section SEM image. It is observed that a gap exists between Pd and Bi_2Te_3. This is the breakage interface due to CTE mismatch between Bi_2Te_3 and alumina. The Ag layer on Bi_2Te_3 was well bonded to the Ag layer on the alumina substrate. On Fig. 4a, it is also found that Pd and Ag atoms have diffused into Bi_2Te_3 by as deep as 5 μm during the annealing process and prior to the bonding. Figure 4b and c display the EDX spectra at locations A and B marked on Fig. 4a. Table 1 provides quantitative EDX data. Location A is in a darker region on the back-scattered electron (BSE) image. The EDX system detects Bi, Te, Ag and Pd. Table 1 shows 54 at.% Ag and 5 at.% Pd. Significant Ag has diffused through Pd into Bi_2Te_3. This makes the Ag diffused region darker on the BSE image because Ag has a smaller atomic number than Bi and Te. The BSE image suggests that Ag has diffused to 5 μm in depth after annealing at 250 °C for 10 h. At location B, which is 7 μm away from the interface, 7 at.% Ag is detected. The small Ag amount does not make the region appear darker on the BSE image. As a result of Ag diffusion, Pd is not a good barrier layer on Bi_2Te_3 to block Ag.

3.2 Ni/Au barrier/bonding layers

Bi_2Te_3 chips were plated with 5 μm Ni, followed by 1 μm Au and 10 μm Ag. Au layer works as an adhesion layer between Ni and Ag. Figure 5a, b, c, and d display SEM images on the Au surface of Bi_2Te_3/Ni (5 μm)/Au (1 μm) and on the Ag surface of Bi_2Te_3/Ni (5 μm)/Au(1 μm)/Ag (10 μm) at low and high magnification, respectively. These images show that the surface of Au and Ag layers are flat and smooth. The surface roughness is less than 1 μm and the grain sizes of electroplated Au and Ag are both smaller than 50 nm. All the electroplated layers are well bonded to each other. Subsequently, the Bi_2Te_3/Ni/Au/Ag samples were annealed at 250 °C for 10 h. Figure 6 displays the cross section SEM image of Bi_2Te_3/Ni (5 μm)/Au (2 μm)/Ag (10 μm) sample after annealing at 250 °C for 10 h. Severe inter-diffusions among Bi_2Te_3/Ni, Ni/Au and Ni/Au/Ag layers are observed. Table 2 presents EDX quantitative data at five locations, A, B, C, D, and E, marked on Fig. 6. The accelerating voltage is 20 keV. These EDX data show inter-diffusions between Bi_2Te_3 and Ag/Au/Ni. At location A, large amount of Ag and Au are detected in the original Ni layer, indicating that Ag and Cu atoms have diffused into the

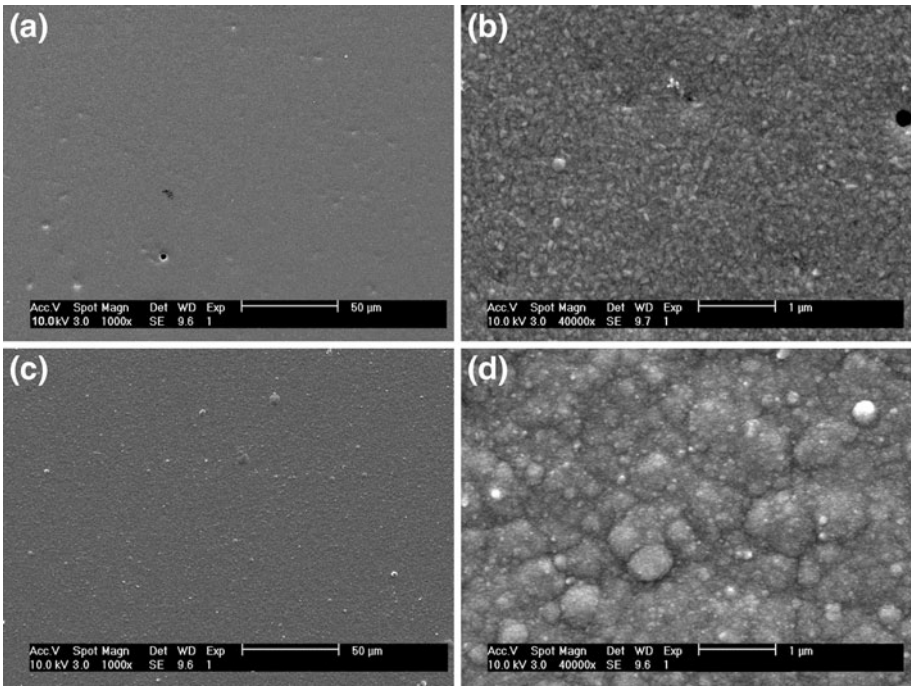

Fig. 5 SEM images on the surfaces of Bi_2Te_3/Ni (5 μm)/Au (1 μm) at **a** low magnification and **b** high magnification, and of Bi_2Te_3/Ni (5 μm)/Au (1 μm)/Ag (10 μm) at **c** low magnification and **d** high magnification

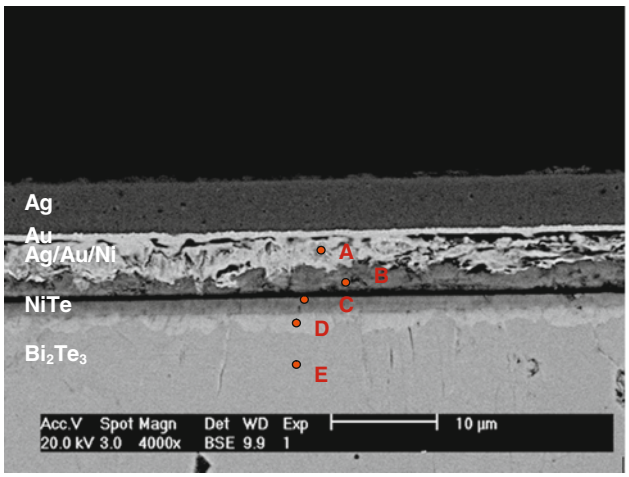

Fig. 6 Cross section SEM image of Bi_2Te_3/Ni (5 µm)/Au (2 µm)/Ag (10 µm) sample after annealing at 250 °C for 10 h. EDX data at locations A, B, C, D, and E are presented in Table 2. Severe inter-diffusions among layers are observed. A compound layer NiTe is formed between Ni layer and Bi_2Te_3. NiTe seems to be mechanically weak. The multilayer structure eventually broke up within NiTe layer due to CTE mismatch

Table 2 EDX quantitative data at location A, B, C, D, and E marked in Fig. 6

Location	At.%				
	Bi	Te	Ni	Au	Ag
A	4	2	13	39	42
B	6	45	46	2	1
C	7	52	38	1	1
D	62	31	5	1	1
E	54	42	2	1	1

The accelerating voltage is 20 kV

Ni layer during annealing. At locations B and C, which are right above and below the breaking interface, respectively, a large quantity of Ni and Te are detected as well as a small amount of Bi. This suggests that Ni and Bi_2Te_3 have inter-diffused, forming NiTe layer [16, 17]. Since the atomic ratio between Ni and Te is around 0.7 ~ 1:1, this layer is probably NiTe compound. Location D and E are basically Bi_2Te_3. The BSE image clearly shows that the breakage incurs inside the NiTe compound. Apparently, NiTe compound is weak and breaks due to stress induced by CTE mismatch in the multilayer structure. Thus, the Ni/Au composite is not a good choice for bonding/barrier layer.

3.3 Ag barrier/bonding layer

This is the simplest design because Ag itself is the electrode. In experiment, 10 µm Ag was electroplated on Bi_2Te_3 chips, followed by annealing at 250 °C for 10 h. Figure 7a and b show the surface of Ag layer on Bi_2Te_3 before annealing at low and high magnification, respectively. The Ag layer bonds well to Bi_2Te_3 and its grain size is less than 50 nm. Figure 8 exhibits the cross section SEM image a Bi_2Te_3/Ag (10 µm) sample after annealing. Severe inter-diffusion between Ag and Bi_2Te_3 is observed. An Ag_2Te compound layer is formed based on EDX analysis and Ag-Bi-Te phase diagram [18]. This layer has some voids and partly breaks off the Bi_2Te_3 chip. It is clear that Ag is not a good barrier/bonding layer for Bi_2Te_3.

3.4 Ti/Au barrier/bonding layers

Bi_2Te_3 were coated with 100 nm Ti and 100 nm Au by an E-beam thermal evaporator and then plated with 20 µm Ag. Figure 9a and b are the SEM images on Au surface of a Bi_2Te_3/Ti/Au sample at low and high magnification, respectively. The Ti (100 nm)/Au (100 nm) layers are well deposited on the Bi_2Te_3 chip with good uniformity. Figure 9c and d show the Ag surface of a Bi_2Te_3/Ti/Au/Ag sample at low and high magnification, respectively. The Ag morphology is different from the Ag plated on other barrier layers. The grains of Ag layer plated on Ti/Au are coarser. The grain size is about 100 nm. Without annealing, a few samples were cut and polished for examinations. Figure 10a and b display the cross section SEM images of a Bi_2Te_3/Ti/Au/Ag sample at low and high magnification, respectively. It is observed that the Ti layer bonds well Bi_2Te_3, the Au layer bonds well to the Ti layer and the Ag layer bonds well to the Au layer. Figure 10b also demonstrates that the Ti/Au

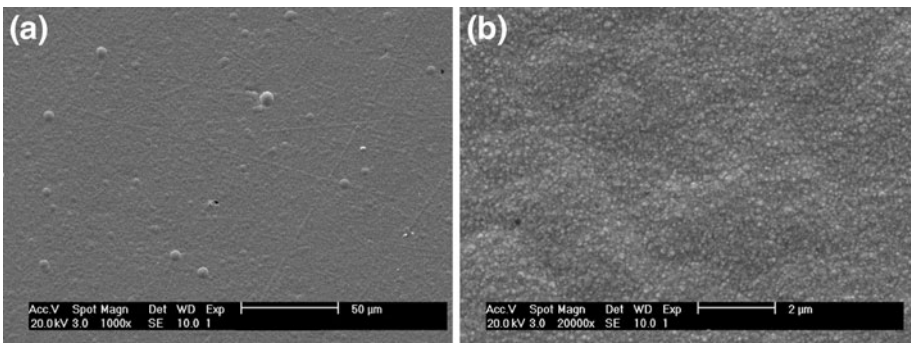

Fig. 7 SEM images on the surfaces of Bi_2Te_3/Ag (10 µm) at **a** low magnification and **b** high magnification

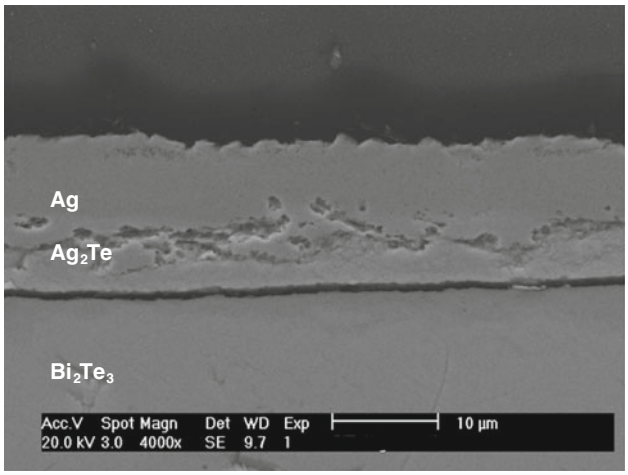

Fig. 8 SEM image on the cross section of Bi_2Te_3/Ag (10 μm) after annealing at 250 °C for 10 h. An Ag_2Te compound layer is formed between Bi_2Te_3 and Ag. It has some voids and partly breaks off the Bi_2Te_3 chip

layers have excellent step coverage over the rough Bi_2Te_3 surface. The Ti/Au layers cover all the steps, jags, and protuberances. Moreover, no Ag or Au atoms diffuse through the Ti layer and get into Bi_2Te_3. Also, no Bi_2Te_3 diffuses through the Ti layer and gets into the Ag layer either.

To further evaluate the barrier/bonding functions of Ti/Au layers, Bi_2Te_3 chips with Ti (100 nm)/Au (100 nm)/Ag (20 μm) were annealed at 250 °C for 50 h. Figure 11a and b exhibit the cross section SEM images of a sample after annealing at low and high magnification, respectively. These BSE images indicate that there is no interdiffusion among Ag, Ti/Au, and Bi_2Te_3 chips. In the Bi_2Te_3 region, no other element traces show up on the contrast of the image. This means that the integrity of Bi_2Te_3 chips is well preserved after the annealing. Moreover, the Ti/Au layers still maintain exceptional step coverage over the rough Bi_2Te_3 surface. They also adhere to the Ag electrode and

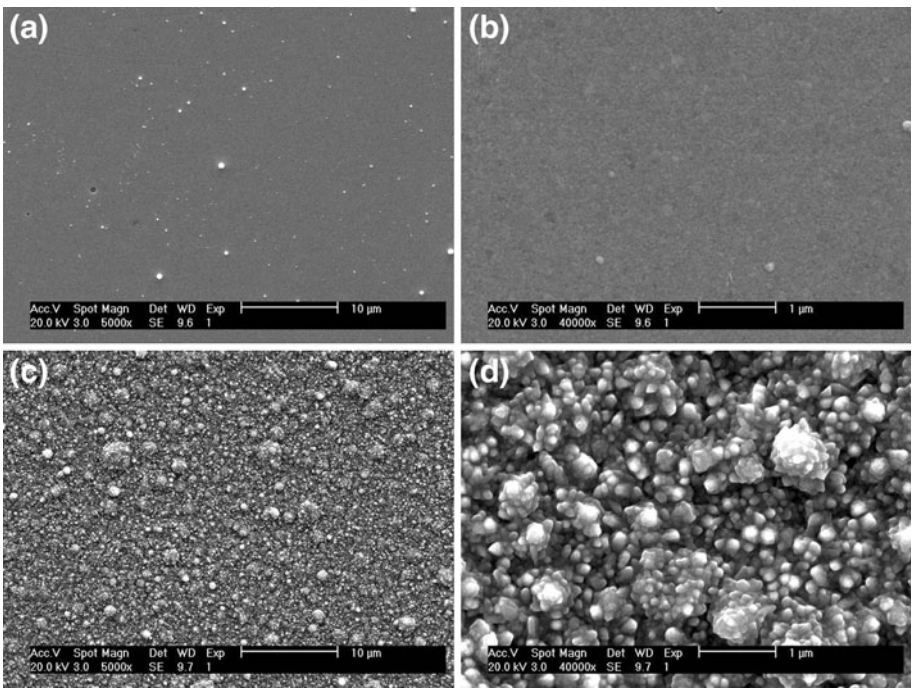

Fig. 9 SEM images on the Au surfaces of Bi_2Te_3/Ti (100 nm)/Au (100 nm) at **a** low magnification and **b** high magnification, and on the Ag surfaces of Bi_2Te_3/Ti (100 nm)/Au (100 nm)/Ag (10 μm) at **c** low magnification and **d** high magnification

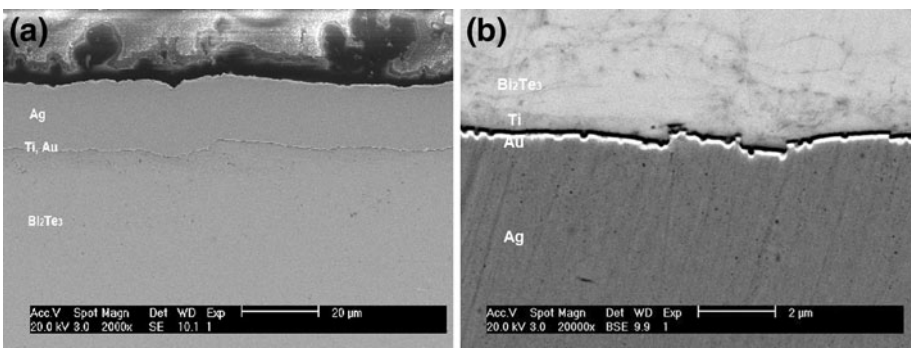

Fig. 10 Cross section SEM images of Bi_2Te_3/Ti (100 nm)/Au (100 nm)/Ag (20 μm) at **a** low magnification and **b** high magnification without annealing. The Ti/Au layers exhibits excellent step coverage on the rough Bi_2Te_3 surface. The Ti/Au layers are continuous and cover the entire Bi_2Te_3 surface with any breakage or pinhole

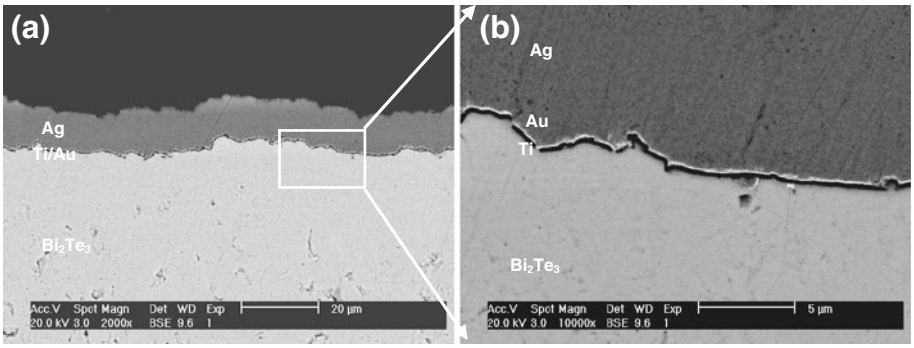

Fig. 11 Cross section back-scattered SEM images of Bi_2Te_3/Ti (100 nm)/Au (100 nm)/Ag (20 µm) sample annealed at 250 °C for 50 h: **a** high magnification and **b** low magnification. The thin Ti/Au layers show exceptional step coverage over the rough Bi_2Te_3 surface even after the annealing

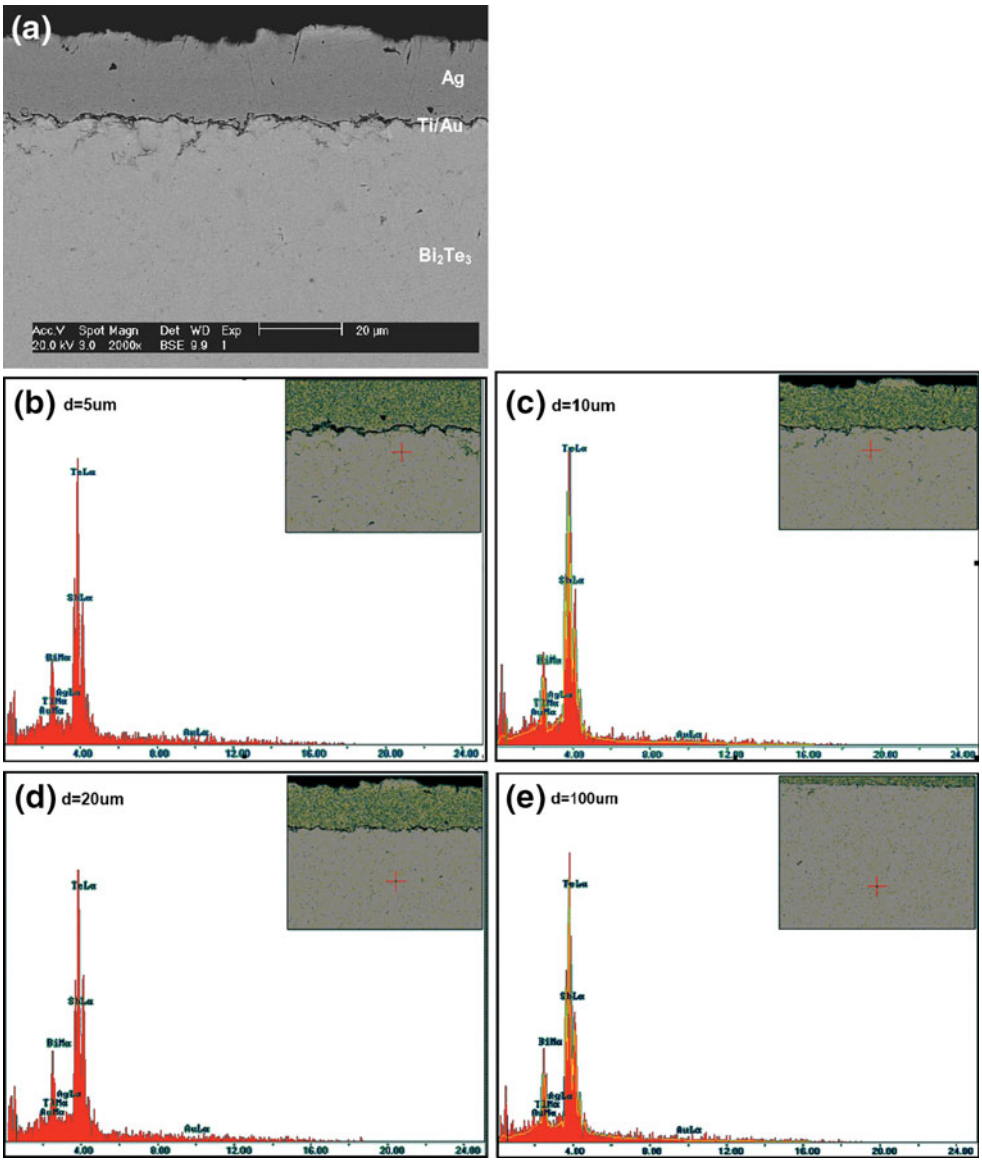

Fig. 12 SEM and EDX evaluation of a Bi_2Te_3/Ti (100 nm)/Au (100 nm)/Ag (20 µm) sample after annealing at 250 °C for 200 h. **a** Cross section SEM, **b**, **c**, **d**, and **e** EDX spectra at locations 5, 10, 20 and 100 µm below the Ti/Au interface with an accelerating voltage 20 keV. EDX quantitative data are provided in Table 3. Again, the Ti/Au layers still keep the excellent step coverage on the rough Bi_2Te_3 surface after the annealing process. No Ag is detected in the Bi_2Te_3 chip

the Bi_2Te_3 chip well. Next, the annealing time was extended to 200 h. Figure 12a exhibits the cross section SEM image of a sample which was annealed at 250 °C for 200 h. No interdiffused region is observed. The thin Ti/Au layers on the SEM image do not appear as sharp as those of the sample annealed for 50 h. But even so, the Ti/Au layers are still continuous and complete. To investigate whether Ag atoms diffuse through the Ti/Au layers and get into Bi_2Te_3 region, EDX analysis was performed on the cross section exhibited in Fig. 12a. Figure 12b, c, d, and e

Table 3 EDX quantitative data of a Bi_2Te_3/Ti (100 nm)/Au (100 nm)/Ag (10 μm) sample at locations in Bi_2Te_3 at depth 5, 10, 20, and 100 μm, respectively, from the Ti/Au interface

Location	At.%			
	Sb	Te	Bi	Ag
d = 5 μm	31	54	9	1
d = 10 μm	34	52	9	1
d = 20 μm	30	54	10	2
d = 100 μm	32	54	9	1

The sample was annealed at 250 °C for 200 h. The accelerating voltage is 20 keV

present the EDX spectra at an accelerating voltage 20 keV at the locations 5, 10, 20, and 100 μm away from the Ti/Au interface. The Sb, Te, and Bi peaks are clearly detected. Sb is there because this is a p-type material. The EDX data are provided in Table 3. At all four locations, the compositions of Sb, Te, and Bi are 30 ~ 34 at.%, 52 ~ 54 at.%, and 8 ~ 10 at.%, respectively. On the EDX spectra, Ag peak is barely seen. The 1 ~ 2 at.% Ag shown in Table 3 is within the error bar of the EDX system. It is thus clear that no Ag atoms diffuse through Ti/Au layers and get into Bi_2Te_3. The Ti/Au layers still work functionally as barrier and adhesion layers. Ti/Au themselves do not diffuse and spread outwards into Ag and Bi_2Te region.

The results presented above illustrate that Ti/Au layers meet the four requirements of barrier/bonding composite design even after annealing at 250 °C for 200 h: (a) prevent Ag and Bi_2Te_3 from inter-diffusion, (b) bond well to Ag, (c) bond well to Bi_2Te_3, and (d) do not themselves diffuse into Bi_2Te_3 and Ag.

4 Summary

We have demonstrated that Ti (100 nm)/Au (100 nm) layers deposited on Bi_2Te_3 chips by E-beam thermal evaporation performs well as bonding/barrier composite between Bi_2Te_3 chips and Ag electrode. After annealing at 250 °C for 200 h, there is no sign of inter-diffusion between Bi_2Te_3 chips and Ag electrode. The Ti/Au layers still bond well to Bi_2Te_3 on one side and Ag on the other. The Ti/Au atoms themselves do not diffuse into Bi_2Te_3 either. Furthermore, the Ti/Au layers provide excellent step coverage on the Bi_2Te_3 surface with a few microns of surface roughness. The coverage is continuous and complete.

Other bonding/barrier composite designs that were experimented with include Pd, Ni/Au, and Ag, respectively. After annealing at 250 °C for 10 h, they diffuse into Bi_2Te_3 to produce alloys or form compounds. The resulting compounds are usually weak and break more easily than other layers in the structure.

Acknowledgments This project was supported by Sandia National Laboratories. Wen P. Lin was partly supported by Materials and Manufacturing Technology fellowship at the University of California, Irvine. Sandia National Laboratories is a multi-program laboratory operated by Sandia Corporation, a wholly owned subsidiary of Lockheed Martin Corporation, for the U.S. Department of Energy's National Nuclear Security Administration under contract DE-AC04-94AL85000.

References

1. R.R. Heikes, R.W. Ure, *Thermoelectricity: Science and Engineering* (Interscience, New York, 1961)
2. F.D. Rosi, Thermoelectricity and thermoelectric power generation. Solid-State Electron **11**, 833–848 (1968)
3. C. Wood, Materials for thermoelectric energy-conservation. Rep. Prog. Phys. **51**, 459–539 (1988)
4. G. Jeffrey Snyder, E.S. Toberer, Complex thermoelectric materials. Nat. Mater. **7**, 105–114 (2008)
5. D.M. Rowe, *Thermoelectrics Handbook: Macro to Nano* (Taylor and Franics Group, New York, 2006), pp. 1–9. ISBN 0849322642
6. E.J. Winder, A.B. Ellis, Thermoelectric devices: solid-state refrigerators and electrical generators in the classroom. J. Chem. Educ. **73**, 940–946 (1996)
7. http://www.inbthermoelectric.com/highperformance.html
8. C.B. Satterthwaite, Electrical and thermal properties of Bi_2Te_3. Phys. Rev. **108**, 1164–1170 (1957)
9. B.W. Howlett, S. Misra, M.B. Bever, Trans. AIME **230**, 1361–1367 (1964)
10. N.Kh. Abrikosov, V.F. Bankina, Kharitonovitch, *Semiconductor Compound and its Properties* (Nauka, Moscow, 1967)
11. Y.C. Lan, D.Z. Wang, G. Chen, Z.F. Ren, Diffusion of nickel and tin in p-type (Bi, Sb)2Te3 and n-type Bi2(Te, Se)3 thermoelectric materials. Appl. Phys. Lett. **92**, 101910 (2008)
12. T. Kacsich, E. Kolawa, J.P. Fleirual, T. caillat, M.-A. Nicolet, Films of Ni-7%, Pd, Pt and Ta-Si-N as diffusion barriers for copper on Bi_2Te_3. J. Phys. D Appl. Phys. **31**, 2406–2411 (1998)
13. O.D. Lyore, T.H. Lee, R.P. Gupta, J.B. White, H.N. Alshareef, M.J. Kim, B.E. Gnade, Interface characterization of nickel contacts to bulk bismuth tellurium selenide. Surf. Interface Anal. **41**, 440–444 (2008)
14. W.P. Lin, P.J. Wang, C.C. Lin. Bonding/barrier layers on bismuth telluride (Bi_2Te_3) for high temperature applications, 60th Electron. Compon. Technol. Conf., pp 447–450 (2010)
15. D. Vasilevskiy, N. Kukhar, S. Turenne, R.A. Masut 2007 "Hot extruded $(Bi,Sb)_2$ $(Te,Se)_3$ alloys for advanced thermoelectric modules". Oral presentation, 5th *European Conference on Thermoelectrics*
16. K. Xiong, W. Wang, H.N. Alshareef, R.P. Gupta, J.B. White, B.E. Gnade, K. Cho, Electronic structures and stability of Ni/Bi_2Te_3 and Co/Bi_2Te_3 interfaces. J. Phys. D Appl. Phys. **43**, 115303 (2010)
17. R.P. Gupta, O.D. Iyore, K. Xiong, J.B. White, K. Cho, H.N. Alshareef, B.E. Gnade, Interface characterization of cobalt contacts on bismuth selenium telluride for thermoelectric devices. Electrochem. Solid-state Lett. **12**, H395–H397 (2009)
18. R. Schmid Fetzer 1988 Ag-Bi-Te phase diagram, ASM Int. (http://www1.asminternational.org/asmenterprise/APD/ViewAPD.aspx?id=950339)